Blazar Jet Emission In The Internal Shock Model Scenario

Authors: Manasvita Joshi[†] and Markus Böttcher (Ohio University)

We explore blazar emission using the internal shock model and multi-zone radiation transfer scheme at sub-pc scales inside its relativistic jet. We follow the time-dependent radiation via synchrotron and SSC processes. Here, we present the effects of varying relevant parameters on the simulated SED and lightcurves of a generic blazar.

Abstract

We use the internal shock model to explore the time-dependent radiation transfer and particle acceleration mechanisms in the inner jet of blazars. We assume a single inelastic collision between a fast and a slow moving plasma shell. The collision results in the formation of a forward and a reverse shock. We consider the instantaneous acceleration of relativistic particles at the two shock fronts, the subsequent radiative cooling of particles, and the resultant self-consistent production of synchrotron and synchrotron self Compton (SSC) radiation. We apply the multi-zone feedback scheme to incorporate the inhomogeneity in the photon density throughout the emission region. Here, we present the effects of varying relevant parameters on the simulated spectral energy distribution (SED) and lightcurves.

Motivation

Blazar jets are highly violent in nature and are dominated by ultrarelativistic particles. The SED of blazars consists of two spectral bumps. The low-energy component is due to synchrotron radiation emanating from relativistic particles, and the high-energy component (for leptonic jet model) is a result of Compton upscattering of the seed photon field by ultrarelativistic particles [1]. The mode of acceleration of plasma electrons (and positrons) to highly relativistic energies and its location in the jet is still not completely understood. One way to comprehend the physics of particle acceleration is the internal shock model, in which the central engine (black hole + accretion disk) spews out shells of plasma with different velocity, mass, and energy. The collision between such shells gives rise to internal shocks (reverse (RS) and forward (FS)), which convert the ordered bulk kinetic energy of the plasma into the magnetic field energy and the random kinetic energy of the particles. The highly accelerated particles then start to radiate and produce the emission observed from the jet.

Internal Shock Model

The collision of two plasma shells results in an emission region as shown in Fig. 1. The treatment of shell collision and shock propagation is hydrodynamic and relativistic in nature [3].
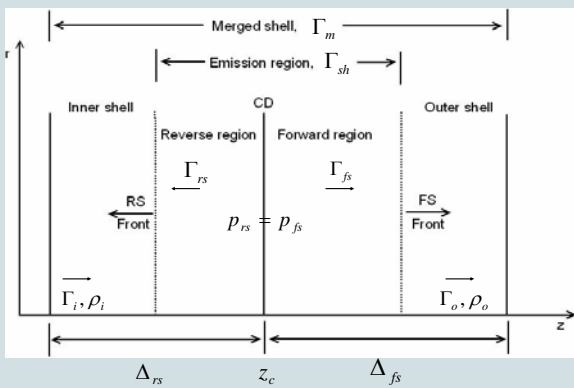

Fig. 1: Schematic of the emission region with RS traveling into the inner shell of BLF, Γ_i, and FS moving into the outer shell with BLF, Γ_o ($\Gamma_i > \Gamma_o$). The pressures of the two shocked fluids, p_{rs} & p_{fs} are the same across the CD. Δ_{rs} & Δ_{fs} are the widths of the inner and outer shell after the collision in the lab frame (central engine frame) obtained from the shock dynamics [1].

Multi-zone Radiation Transfer Scheme

A cylindrical emission region has been considered to calculate the resultant spectrum in a time-dependent manner. The average photon escape timescale needed to carry out such calculation has been obtained semi-analytically by using Eqn. 1 (Fig. 2) [2]. The inhomogeneity in the photon and particle density throughout the emission region has been considered by dividing the region into multiple zones (Fig. 3) [2]. The radiation transfer (Eqn. 2) has been considered within each zone and in between the zones.
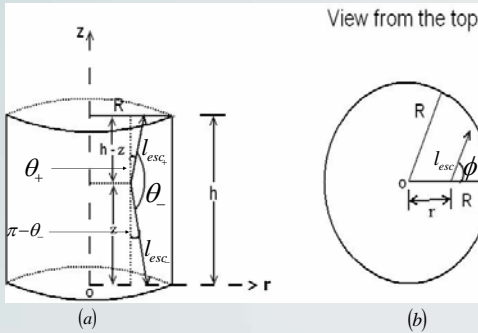

Fig. 2: (a) Depiction of the three possible directions (forward, backward & sideways) of escape for photons from a cylinder. L_{esc+} is the escape length for the forward direction making an angle with the axis of the jet (z-axis), & l_{esc-} is that for the backward direction.

(b) Projection of the escape path length on the horizontal surface.

$$\langle t_{ph,esc} \rangle = \frac{1}{4\pi c} \int_0^{2\pi} d\phi \left[\int_{-1}^{\mu_{crit_-}} l_{esc_-}(\theta,\phi;r,z)d\mu + \int_{\mu_{crit_-}}^{\mu_{crit_+}} l_{esc}d\mu + \int_{\mu_{crit_+}}^{+1} l_{esc_+}d\mu \right] \quad (1)$$
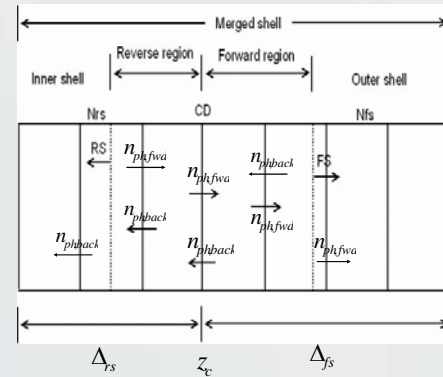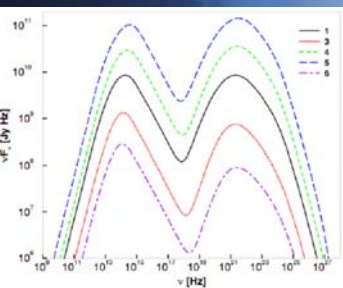

Fig. 3: Schematic of the radiation transfer in between the zones using appropriate photon escape probability functions.

$$dn_{ph,fwd} = n_{ph}\frac{dt}{t_{ph,esc}}P_{fwd} \quad (2)$$

Parameter Study

Table 1

Shell Parameter	Value	Run Number
Outer Shell BLF, Γ_i	22	3 , 4
Outer Shell BLF, Γ_o	18	5 , 6

Fig. 4: Simulated time-integrated SED of a generic blazar illustrating the effects of varying Γ_i (runs 3 & 4), and Γ_o (runs 5 & 6), acc. to Table 1.

Table 2

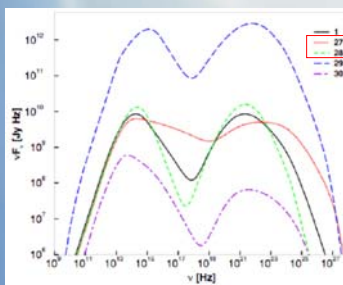| Emission Region Parameter	Value	Run Number
Particle Injection Index, q	3.4	27 , 28
Zone/Jet Radius, R	3×10^{16} cm	29 , 30

Fig. 5: Simulated time-integrated SED of a generic blazar showing the effects of varying q (runs 27 & 28), and R (runs 29 & 30), acc. to Table 2.
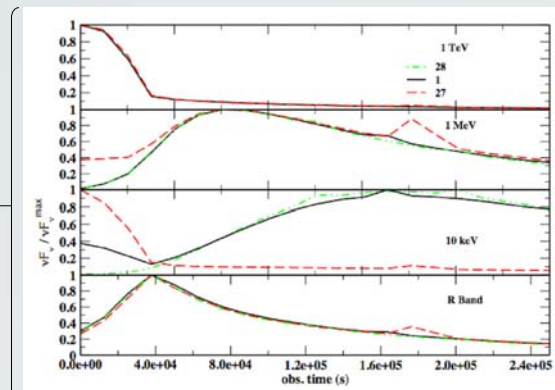

Fig. 6: Simulated lightcurves in various energy bands showing the effects of varying q (runs 27 & 28). Harder energy distribution (smaller q) of the e- population in the region results in a sharper rise & a steeper decline of the acceleration pulse (run 27). The e-s lose their energy faster and more energetic synchrotron photons (X-ray) are produced first in comparison to the lower energy (optical) ones. Thus, rise in the pulse of higher energy bands is sooner in lightcurves resulting from run 27 as compared to those of run 1 and 28.

[1] Böttcher & Schlickeiser, R., 1997, A&A, 325, 866, [2] Joshi & Böttcher, 2009, in preparation, [3] Spada et al., 2001, MNRAS, 325, 1559

† Currently at Boston University

This research is partially supported by NSF Grant AST-0907893